chemistry proceedings

MDPI

Proceeding Paper

Study on the Effect of Applying Benzimidazole–Ethanol Solution as a Film–Forming Corrosion Inhibitor on the Surface of Aluminium Alloy 2024-T3 †

Magdi Hassn Mussa [1,2,3,*], Sarra Takita [4], Farah Deeba Zahoor [4,5], Oliver Lewis [4] and Nicholas Farmilo [4,6]

[1] Mechanical and Energy Department, The Libyan Academy of Graduate study, Tripoli P.O. Box 79031, Libya
[2] Mechanical Engineering Department, Sok Alkhamis Imsehel High Tec. Institute, Tripoli P.O. Box 79034, Libya
[3] The Institute of Marine Engineering, Science and Technology, London SW1H 9JJ, UK
[4] Materials and engineering Research institute MERI, Sheffield Hallam University, Howard Street, Sheffield S1 1WB, UK; Sarah.a.takita@gmail.com (S.T.); F.Zahoor@sheffield.ac.uk (F.D.Z.); O.Lewis@shu.ac.uk (O.L.); nfarmilo@gmail.com (N.F.)
[5] Department of Chemistry, University of Sheffield, Sheffield S3 7HF, UK
[6] Tideswell Business Development Ltd., Ravensfield Sherwood Rd, Buxton SK17 8HH, UK
* Correspondence: magdimosa1976@gmail.com; Tel.: +44-7404496955
† Presented at the 25th International Electronic Conference on Synthetic Organic Chemistry, 1–30 November 2021; Available online: https://ecsoc-25.sciforum.net/.

Abstract: The Al-Cu-Mg light alloys' storage characteristics are such that their use for building structures, marine offshore applications, and aeroplane components, with excellent strength/weight ratios, would not be possible without adherent anticorrosion preservation. Many techniques and strategies are still being used to treat the surfaces, such as cladding, anodising, and greasing. However, due to their costly and time-consuming nature, these techniques are considered complicated. Therefore, volatile organic inhibitor components are now being used effectively. Benzimidazole (BZI) and its derivatives are one of these film-forming chemicals used on copper and steel, directly or as injectables, combined with other carriers, such as fatty acids or dissolvable hydrocarbons, with highly efficient corrosion protection. Therefore, this paper will investigate the enhancement of the corrosion protection afforded by direct spraying of BZI solution on the surface of aluminium alloy AA 2024-T3 The corrosion protection performance results from the high electronegativity of BZI as a film-forming inhibitor, which will be adsorbed on the metallic surface, as it may emulate active protection. The corrosion protection properties of the BZI film-forming coating were preliminarily studied with 3.5% NaCl by using electrochemical impedance testing and simulations. The surface chemical adsorption confirmation was carried out by infrared spectroscopy (ATR-FTIR), supported by analysing the morphology of the surface before and after the immersion testing by using scanning electron microscopy (SEM) real-time imaging within one week of immersion. The benzimidazole film-forming coating exhibited good anticorrosion properties, providing an adherent protection film on AA 2024-T3 samples comparing with bare cladded AA 2024-T3, with a cost-effective and easy application process.

Keywords: volatile corrosion inhibitor; corrosion; adsorption; film-forming chemicals; AA 2024-T3

Citation: Mussa, M.H.; Takita, S.; Zahoor, F.D.; Lewis, O.; Farmilo, N. Study on the Effect of Applying Benzimidazole–Ethanol Solution as a Film–Forming Corrosion Inhibitor on the Surface of Aluminium Alloy 2024-T3. *Chem. Proc.* **2021**, *8*, 14. https://doi.org/10.3390/ecsoc-25-11635

Academic Editor: Julio A. Seijas

Published: 12 November 2021

1. Introduction

Keeping and storing construction components on project sites require exceptional management and preservation to avoid damage and corrosion. Usually, metallic elements are more affected by the environment than other construction materials. Although they are still desirable due to their mechanical properties, especially steel, copper, and aluminium alloys, many preservation procedures could be applied in the factory and on site to reduce the effects of the surrounding environment [1].

The aluminium alloy 2xxx series is desirable for aerospace and marine offshore construction projects due to its strength–weight ratio. Despite that, the aluminium alloy series is susceptible to corrosion more than pure aluminium due to micro-galvanic effects and pitting corrosion caused by the presence of copper-containing intermetallic particles (IMPs), which disrupt the passivating aluminium oxide film on the alloy surface [2]. The different types of IMPs have specific behaviours and electrochemical natures. These ionised phases include iron, manganese, and silicon, which are considered impurities, and IMPs can create cathodic compounds consistent with aluminium itself.

The pitting corrosion mechanism generally consists of two stages, which are initiation and propagation. In the presence of chloride ions on the oxide-passive film on an alloy, the weakest points on the passive oxide film will occur where some intermetallic particles (IMPs) are near the surface. Pitting corrosion will initiate and possibly grow depending on the local conditions, the alloy, and the electrolyte. In many cases, if the pit remains active, then it will involve an internal micro-galvanic cell. It will result in propagation, based upon physically separated aluminium oxidation and oxygen or hydrogen reduction, depending upon the electrode potential of metal and the solution. The following equations can briefly describe the mechanism of pitting corrosion on the AA2024-T3 alloy in aerated neutral and alkaline solution [3]:

$$O_2 + 2H_2O + 4e^- \rightarrow 4OH^- \quad (1)$$

$$O_2 + 4H^+ + 4e^- \rightarrow 2H_2O \quad (2)$$

$$2H^+ + 2e^- \rightarrow H_2 \quad (3)$$

$$H_2O + 2e^- \rightarrow 2OH^- + H_2 \quad (4)$$

$$Al^{3+} + 3H_2O \rightarrow Al(OH)_3 + 3H^+ \quad (5)$$

$$2Al \rightarrow 2Al^{3+} + 6e^- \quad (6)$$

The creation of H^+ will occur as a result of the re-hydrolysis of aluminium ion Al^{3+}, and this will lead to acidify the media around the pit and decrease the pH to lower than 3 pH. Therefore, from Equation (6), because the solution was acidified inside the pit, the local environment will become more aggressive, causing Al dissolution. However, the process continues, hence causing the autocatalytic propagation of the pit. Figure 1 shows a schematic of the mechanism of pitting in the aluminium–copper-based alloys.

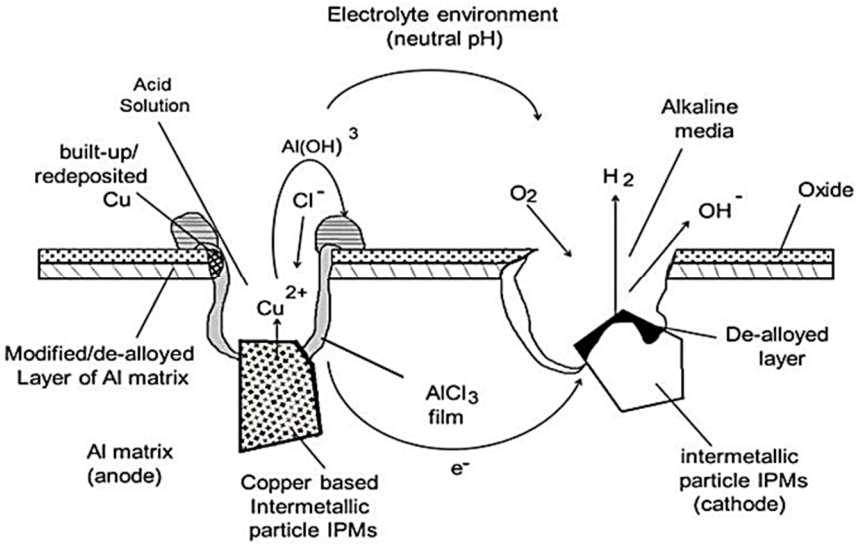

Figure 1. Schematic mechanism of pitting corrosion on aluminium AA2024 [4].

The figure illustrates the common mechanism of pitting in the AA2024-T3 alloy, resulting from the presence of intermetallic particles, which cover about 3% to 4% of the

overall surface area. A majority of these (approximately 60%) IPMs are (Al_2MgCu) S-phase-saturated solid solutions [5,6]. This S-phase is mainly responsible for the corrosion on this alloy because it is more electrochemically active (anodic) than the alloy itself. The electrochemical dissolution of Al and Mg from the S-phase will start during the initial stages of the corrosion process, leaving behind copper, which accumulates on the side of pits as a thin film due to the continuous dissolution of the remaining copper [7]. This thin film of copper around the pits is crucial in developing the localised and micro-galvanic corrosion, causing a growth in the cathodic area and increasing the anodic current density in the pit. Thus, suppressing the S-phase dealloying and deposited copper on AA2024 alloys will positively affect any localised-corrosion-inhibition strategy.

Many techniques for preservation, such as cladding with a thin film of pure aluminium or copper, improve its surface corrosion protection [8,9]. Alternatively, organic inhibitors that can either react with IPMs and S-phase will provide a robust inhibition process [10,11].

Today there is a wide range of volatile inhibitor formulations that may be used for corrosion protection of both ferrous or non-ferrous metals, such as benzimidazole, 2-benzimidazolethiol, and 2-mercaptobenzothiazole; these have been reported as effective inhibitors on copper, steel, zinc, and their alloys [11]. As benzimidazole (BZI) is a imidazole derivative that has been identified as a low-pH film-forming corrosion inhibitor with the structure of a heterocyclic aromatic organic compound, it could be used as both effective VCI or injectable inhibitor with other soluble carriers due to the chemical structure that contains a benzene group. Additionally, the active group of imidazole can be used in the oil and gas industry by using inhibitors-injection pumps [12]. Generally, it has been found that the BZI and its derivatives may be seen in this inhibitor molecule, positioned in a parallel adsorption arrangement, and there was a close joining with the surface [13,14]. In addition, BZI is available commercially as a raw material for many applications, the primary use being in pharmaceutical applications for use as a fungicide [15].

This paper will study the enhancement of corrosion protection that could be provided by spraying an ethanol solution of benzimidazole on aluminium alloys 2024-T3 in a standard 3.5% NaCl solution.

2. Experimental and Work Procedure

2.1. Substrate Preparation and Film Deposition

The commercially aluminium alloy AA2024-T3 Q-panels made with dimensions of (102 mm × 25 mm × 1.6 mm) were purchased from Q-Lab for use as test substrates [16]. First, the received Q-panels were washed with a commercial aluminium-based surfactant cleaner and then rinsed with DI water; after that, they were rewashed with acetone to remove organic residues on the surface. Then, the BZI solution was sprayed, "which is pre-prepared from 1:3 v/v BZI and Ethanol", onto the precleaned aluminium alloy substrates over three phases. After that, the coated samples were left in the air for 10 min. The BZI-treated samples were labelled as BZI-AA 2024, and the other nontreated sample was labelled as Bare-AA 2024.

2.2. Coating Testing and Characterisation

Electrochemical tests were performed on the coatings to assess their corrosion resistance. Tests were conducted by using a Princeton Applied Research PARSTAT. The corrosion performance was evaluated using potentiodynamic polarisation scans (PDPS), and electrochemical impedance spectroscopy (EIS) on the BZI-coated and uncoated aluminium alloy samples. The tested area was 1.00 cm^2 in the centre of the samples in an aerated 3.5% NaCl solution. The tests were carried out at room temperature (20 °C ± 2 °C). Prior to polarisation, the electrode potential was monitored for approximately 1 h in electrolyte solution until stability. The sample was polarised with PDPS at a scan rate of 1.667 mVs^{-1} from the initial potential of −250 mV vs. OCP to +750 mV vs. SCE. The electrochemical impedance measurements were recorded between 100 kHz and 10 MHz with a sinusoidal AC RMS value of 10 mV [17,18].

3. Results and Discussion

3.1. The Potentiodynamic Polarisation Scans (PDPS)

The corrosion and corrosion protection for the bare and treated BZI-AA2024 samples was investigated by potentiodynamic polarisation in the standard NaCl solution, as is shown in Figure 2. The anodic and cathodic behaviour was measured between −250 mV and 750 mV against the tested sample's open circuit potential (OCP). As shown Figure 2, by using Tafel exploiting, the bare AA2024 sample has a corrosion current of 6.9×10^{-6}A/cm^2. The anodic branch of the uncoated sample shows the continuous active dissolution of the metal, while the cathodic branch exhibits diffusion control. The corrosion current density (I_{corr}) of the pre-treated benzimidazole sample BZI-AA2024 is about one order of magnitude lower than the untreated bare-AA2024 sample, with the result at about 5.1×10^{-7}A/cm^2.

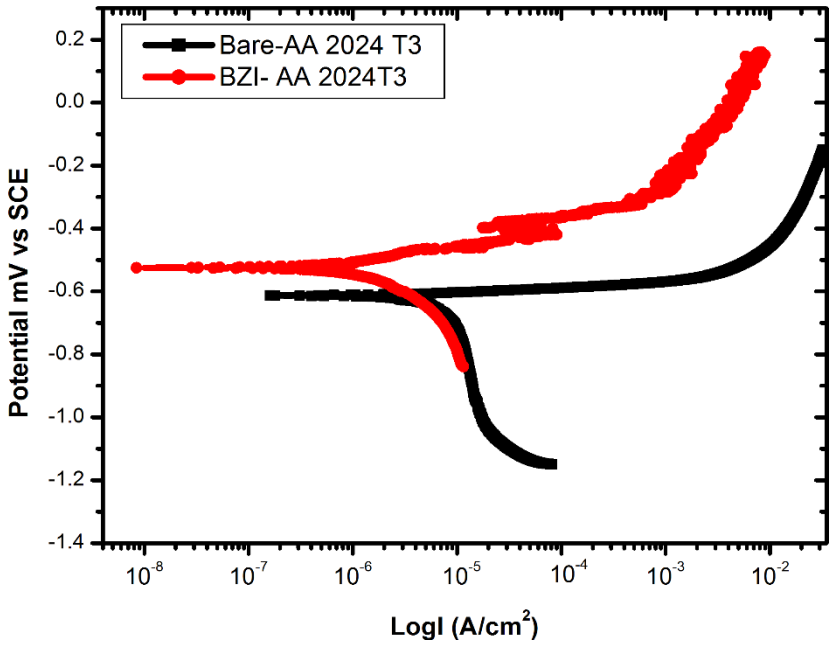

Figure 2. (PDPS) Polarization curves for the bare and BZI-coated samples in 3.5% NaCl.

The corrosion potential of bare AA2024 was measured at -612 ± 2 mV(SCE), while the BZI-AA2024 was measured at -565 ± 2 mV(SCE) respectively. The cathodic branches showed different diffusion control on all treated samples. The pitting potential of BZI bare AA2024 was about −500 mV suggests that the pitting may here be commenced. The cathodic branch of the BZI treated sample was stabilized with one order of magnitude lower than the Bare. Table 1 shows the summarised PDPS polarisation data.

Table 1. PDPS polarisation data for both samples.

Sample	E_{corr} [mV] (Vs. SCE)	I_{corr} [A/cm^2]	Average OCP mV vs. SCE
Bare-AA2024	-612 ± 2	6.9×10^{-6}	610
BZI-AA2024	-565 ± 2	5.1×10^{-7}	615

3.2. The Electrochemical Impedance Spectroscopy (EIS)

The EIS impedance data for the bare and BZI-AA2024 samples; run-in period of the 144 h immersion test is shown in Figure 3. Starting from one hour of immersion of the bare-AA2024, a low impedance of about 3 ohms.cm^2 was observed at high frequencies between 10^3 and 10^5 Hz. This is attributed to surface interface and solution resistance. Furthermore, it slightly decreased to about 2.6 ohms.cm^2 after 144 h immersion at a low frequency from 0.1 to 0.01 Hz; the impedance generally decreased from the 1 h to 144 h.

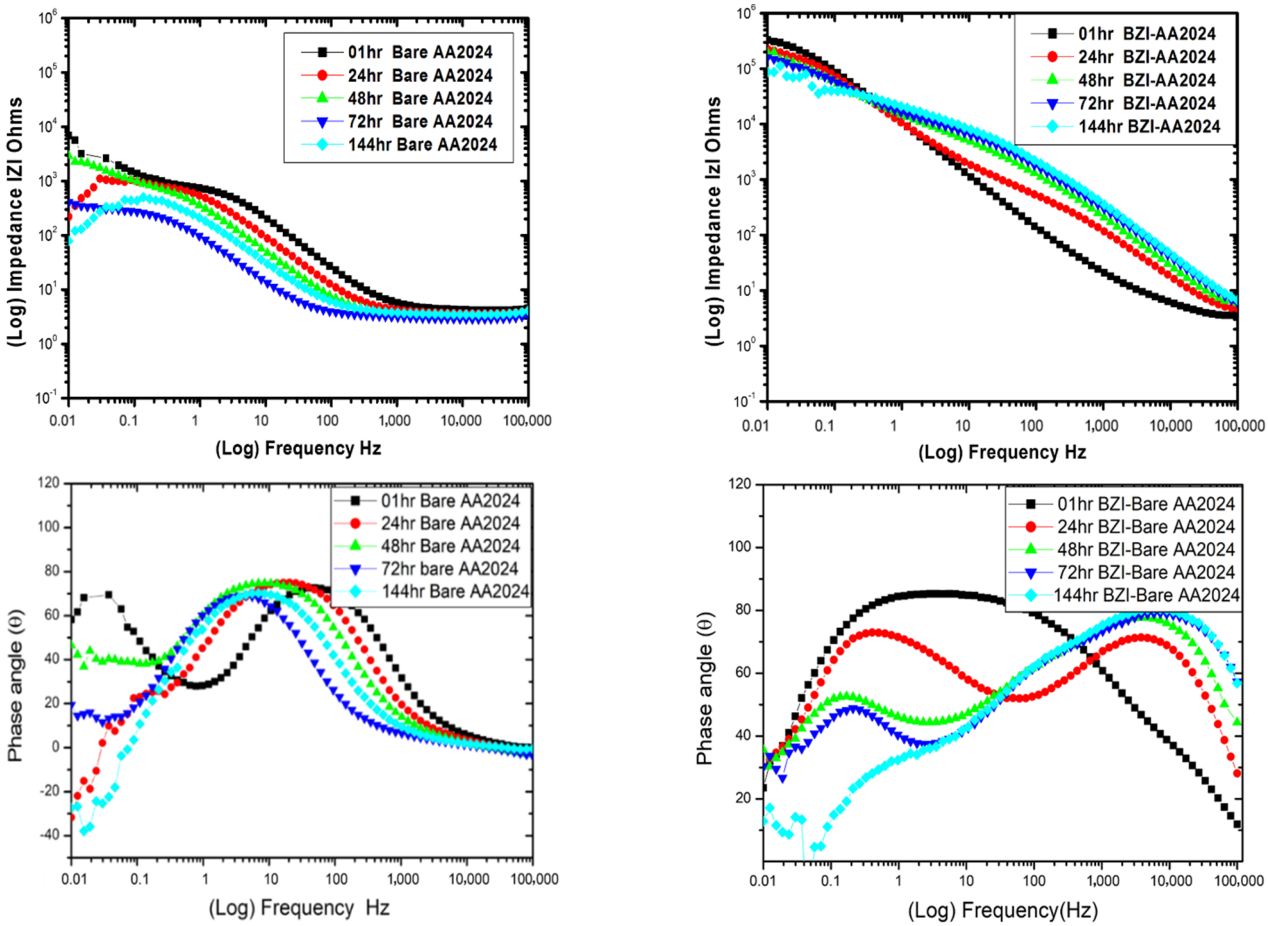

Figure 3. Impedance behaviour and phase angle response of bare and BZI-coated AA2024 in 3.5% NaCl solution.

The impedance data for the BZI-AA2024 substrate, as shown in Figure 3, show the EIS results after one hour of immersion-exposed nominal impedance, starting at about 8ohms.cm^{-2}, that might be attributed to surface interface solution resistance at high frequencies between 10^5 and 10^3 Hz. Then, it starts to rise with slight sloping to reach the higher magnitude in the low frequencies between 1.0 and 0.01 Hz with a value of about 3.3×10^5ohms.cm^{-2}, which is higher by two orders of magnitude than the bare-AA2024 sample. However, from 24 h to 144 h, two time constants were observed, the first time constant started between 10^5 and 10^3 Hz, and the second began between 10 and 0.1 Hz. These two time constants could be attributed to the integration of BZI film and the aluminium oxide film on the substrate.

After 24 h of the immersion period, it continued to behave similarly as a coated sample, which shows a degree of protection. At low frequencies from 0.1 to 0.01 Hz, the impedance decreased dramatically from the 1 h to 144 h to reach about 2.0×10^5ohms.cm^{-2}. This suggests the possibility of creating a film of benzimidazole on the substrate to save the AA2024-T3 alloy from direct corrosion. Furthermore, the phase angle θ plot for BZI - AA2024 showed one big time constant in the first immersion hour, between 10^3 and 0.1 Hz; these are attributed to the created BZI film layer, which came from the sample-treatment process. After 24 h, until 144 h, it showed two time constants, which shifted from around 100 Hz to around 10 Hz. These two time constants could be attributed to the integration of BZI film and the aluminium oxide film on the substrate. Meanwhile, the bare-AA2024 maintained a time constant from 1 h to 144 h.

3.3. Chemical Composition and Adsorption Confirmation

3.3.1. Energy-Dispersive X-ray Spectroscopy (EDX)

The trace of the benzimidazole after 144 h of testing in 3.5% NaCl on the surface of AA 2024-T3 substrate was checked by using the EDX technique. By using EDX analysis, as shown in Figure 4a,b, the spectrum showed a minimal trace of nitrogen, which reflects the presence of an azole group on the surface. By zooming in, the spectrum from 0.1 to 2.0 KeV shows the peak shoulder, which confirms the nitrogen at about 0.4 KeV by element weight percentage of 1.0~1.1 wt.% [19].

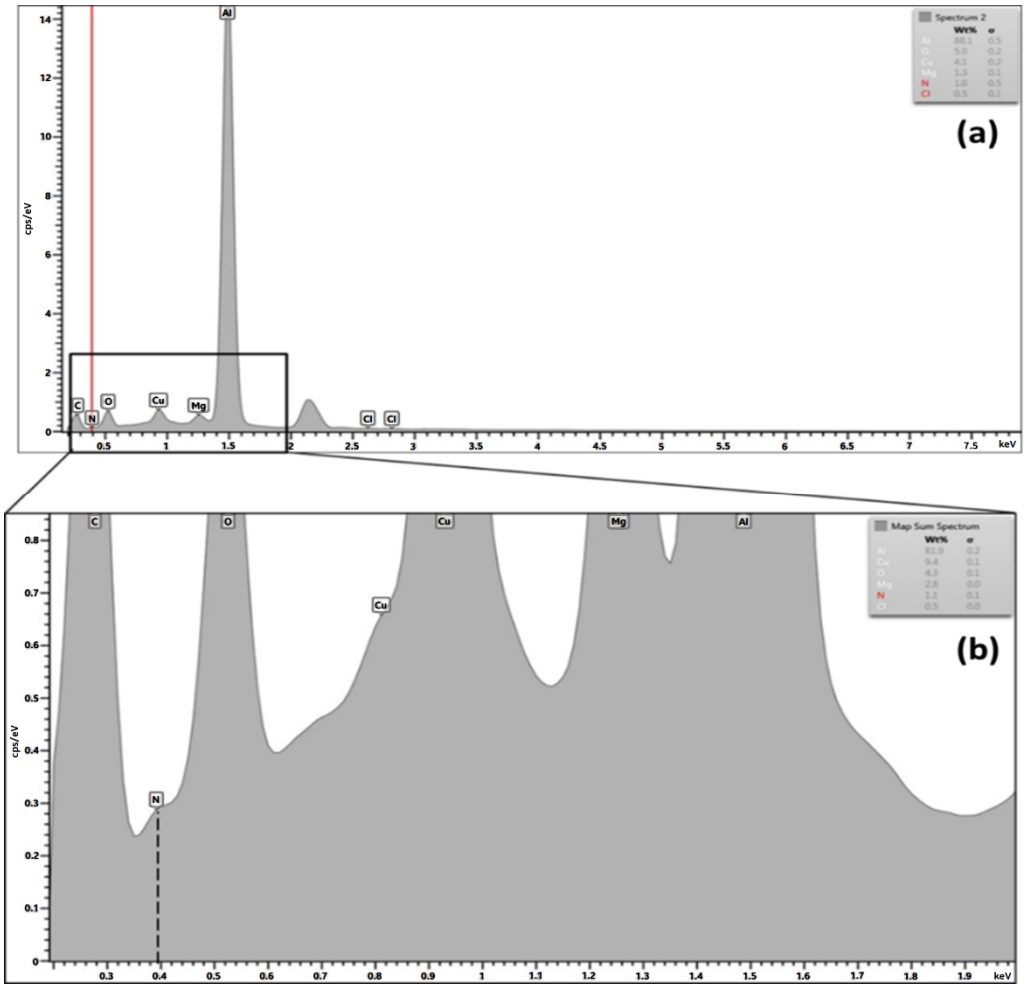

Figure 4. (**a**) EDX spectrum; (**b**) zoomed spectrum showing the trace of nitrogen adsorption on the AA2024-T3 after 144 h of immersion.

3.3.2. ATR-FTIR Data Analysis of Chemical Confirmation

FTIR data confirm the presence of benzimidazole (BZI) film adsorption on the surface of AA2024-T3 substrate before and after immersion. The benzimidazole FTIR is carried out as a control and is presented in Figure 5. Numerous vibration modes are characteristic of the BZI molecule. Additionally, these peaks and stretches can be observed and remain on the BZI-AA2024 sample after treatment. The imine C=N stretching is present at 1588 cm^{-1}, and additional carbon double bond, C=C, stretching peaks are confirmed at 1478 cm^{-1}, 1459 cm^{-1}, and 1410 cm^{-1}, respectively.

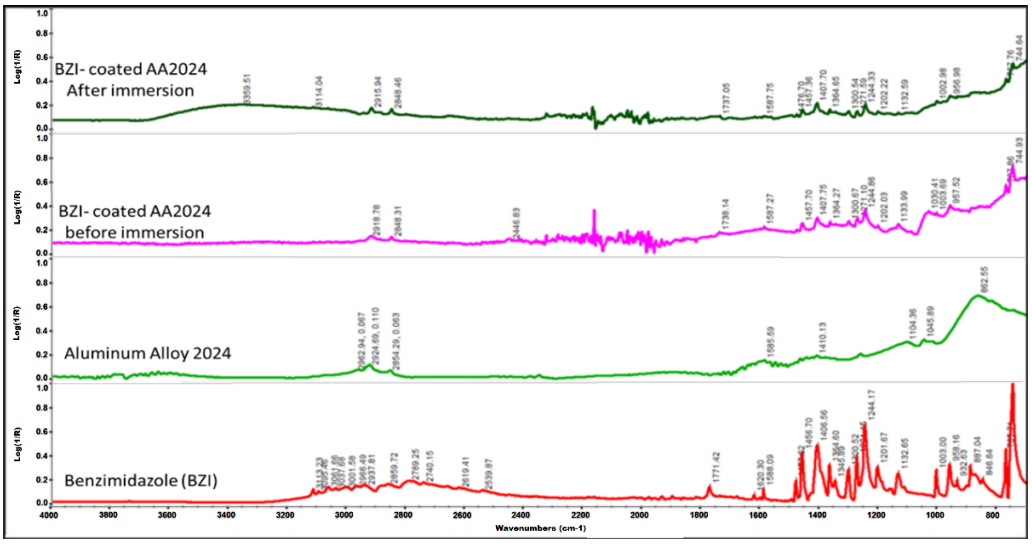

Figure 5. Contact mode ATR spectrum for BZI-AA2024 sample before and after immersion in 3.5% NaCl solution.

Likewise, the fingerprint of the aromatic amine stretching C-N can be detected at 1365, 1348, and 1302 $cm^{-1,}$ respectively, confirming the benzimidazole presence on the substrate. These stretching peaks keep their position even after long immersion periods, which might be attributed to the BZI reacting with a metallic surface. A weak group of peaks characterise the C-H out-of-plane bending at 958,885,769 and 750 cm^{-1} [20].

Although, there was a trace of adsorption of benzimidazole after 144 h of immersion, with hydration taking place due to diffusion action; as a result of this, OH-stretching appears at low intensity in the region between 3000 and 3400 cm^{-1}, which can be attributed to aluminium hydroxide Al-OH film and the remaining propagated H_2O in the interfacial and oxidised layers [21,22].

3.4. Scanning Electron Microscopy Images (SEM)

Figure 6 shows the surface morphology of both samples, BZI-AA2024 and bare alloy AA. It is clear that the bare sample is attacked by pitting corrosion after long immersion of 144 h, as showed in Figure 6a. On the other hand, the BZI coated sample showed excellent resistance to corrosion under similar circumstances, as seen in Figure 6b. Furthermore, the measurements showed that the Benzimidazole was more stable in the salty water, 3.5% NaCl, which may be attributed the prevention of the diffusion in the coating system, in line with the benzimidazole self-healing-inhibition properties.

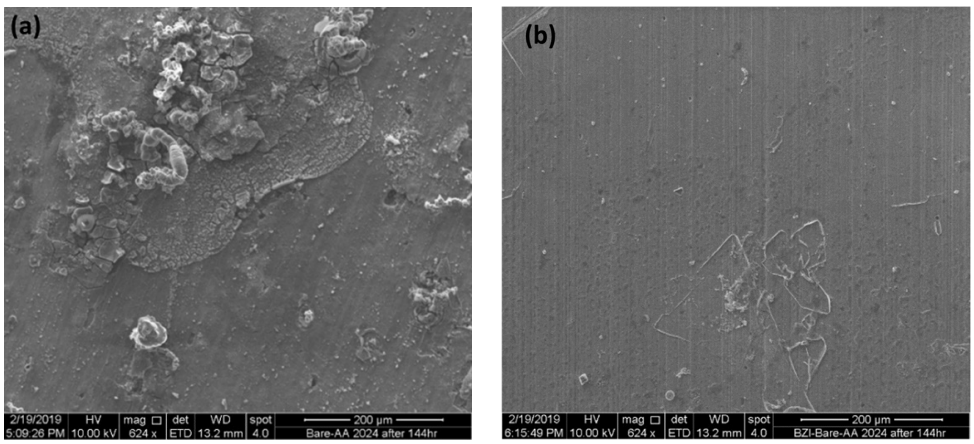

Figure 6. Shows a SEM images of the bare (**a**) and BZI-AA2024 (**b**) samples after immersed in 3.5% NaCl solution.

4. Conclusions

Through electrochemical testing techniques, we evaluated the spraying of the benzimidazole solution on aluminium alloys 2024-T3, which revealed excellent corrosion protection when combined with the nontreated sample, which can provide protection over one week without any failure or pitting signs on the surface in an aggressive medium of 3.5% NaCl. Furthermore, applying benzimidazole as a film-forming inhibitor on the surface provides simulated active protection due to the high electronegativity of the active azole group. Additionally, it gains the highest impedance when compared with the noncoated AA 2024-T3 as. This is a cost-effective alternative: BZI could be used instead of the traditional short-term ways of storing aluminium alloys.

Author Contributions: All authors contribute equally. All authors have read and agreed to the published version of the manuscript.

Funding: This research received no external funding.

Institutional Review Board Statement: Not applicable.

Informed Consent Statement: Not applicable.

Data Availability Statement: The data are not publicly available; the files are stored on correspond.

Acknowledgments: The authors would like to acknowledge the Libyan scholarship programme and materials and engineering research institute (MERI) at Sheffield Hallam University for facilitating support.

Conflicts of Interest: The authors declare no conflict of interest.

References

1. Tiringer, U.; Kovač, J.; Milošev, I. Effects of mechanical and chemical pre-treatments on the morphology and composition of surfaces of aluminium alloys 7075-T6 and 2024-T3. *Corros. Sci.* **2017**, *119*, 46–59. [CrossRef]
2. Boag, A.; Hughes, A.E.; Glenn, A.M.; Muster, T.H.; McCulloch, D. Corrosion of AA2024-T3 Part I: Localised corrosion of isolated IM particles. *Corros. Sci.* **2011**, *53*, 17–26. [CrossRef]
3. Vargel, C. *Corrosion of Aluminium*, 1st ed.; ELSEVIER SCIENCE B.V: Oxford, UK, 2004.
4. Mussa, M. Development of Hybrid Sol-Gel Coatings on AA2024-T3 with Environmentally Benign Corrosion Inhibitors. Ph.D. Thesis, Sheffield Hallam University, Sheffield, UK, 2020.
5. Polmear, I.; StJohn, D.; Nie, J.-F.; Qian, M. Physical metallurgy of aluminium alloys. In *Light Alloys*; Butterworth-Heinemann, Elsevier Ltd.: Oxford, UK, 2017; pp. 31–107. ISBN 9780080994314.
6. Wang, S.C.; Starink, M.J. Precipitates and intermetallic phases in precipitation hardening Al–Cu–Mg–(Li) based alloys. *Int. Mater. Rev.* **2005**, *50*, 193–215. [CrossRef]
7. Buchheit, R.G.; Grant, R.P.; Hiava, P.F.; Mckenzie, B.; Zender, G. 1. Local Dissolution Phenomena Associated with S Phase (AI2CuMg) Particles in Aluminum Alloy 2024-T3. *J. Electrochem. Soc.* **1997**, *144*, 2621. [CrossRef]
8. Okafor, A.C.; Nnadili, C. Evaluation of the Effects of Corrosion on Fatigue Life of Clad Aluminum Alloy 2024-T3-Riveted Lap Joints with Acoustic Emission Monitoring. *J. Fail. Anal. Prev.* **2012**, *12*, 670–682. [CrossRef]
9. Mussa, M.H.; Rahaq, Y.; Takita, S.; Farmilo, N. Study the Enhancement on Corrosion Protection by Adding PFDTES to Hybrid Sol-Gel on AA2024-T3 Alloy in 3.5% NaCl Solutions. *Albahit J. Appl. Sci.* **2021**, *2*, 61–68.
10. Andreev, N.N.; Kuznetsov, Y.I. Volatile inhibitors of metal corrosion. I. vaporization. *Int. J. Corros. Scale Inhib* **2012**, 16–25. [CrossRef]
11. Bastidas, D.M.; Cano, E.; Mora, E.M. Volatile corrosion inhibitors: A review. *Anti-Corrosion Methods Mater.* **2005**, *52*, 71–77. [CrossRef]
12. Wright, J.B. The Chemistry of the Benzimidazoles. *Chem. Rev.* **1951**, *48*, 397–541. [CrossRef] [PubMed]
13. Obot, I.B.; Madhankumar, A.; Umoren, S.A.; Gasem, Z.M. Surface protection of mild steel using benzimidazole derivatives: Experimental and theoretical approach. *J. Adhes. Sci. Technol.* **2015**, *29*, 2130–2152. [CrossRef]
14. Gutiérrez, E.; Rodríguez, J.A.; Cruz-Borbolla, J.; Alvarado-Rodríguez, J.G.; Thangarasu, P. Development of a predictive model for corrosion inhibition of carbon steel by imidazole and benzimidazole derivatives. *Corros. Sci.* **2016**, *108*, 23–35. [CrossRef]
15. Gupta, P.K. Herbicides and fungicides. In *Biomarkers in Toxicology*; Elsevier Inc.: Amsterdam, The Netherlands, 2014; pp. 409–431. ISBN 9780124046306.
16. Mussa, M.H.; Farmilo, N.; Lewis, O. The Influence of Sample Preparation Techniques on Aluminium Alloy AA2024-T3 Substrates for Sol-Gel Coating. *Eng. Proc.* **2021**, *11*, 5. [CrossRef]
17. Tait, W.S. *Electrochemical Impedance Spectroscopy Fundamentals, an Introduction to Electrochemical Corrosion Testing for Practicing Engineers and Scientists*; Tait, W.S., Ed.; PairODocs Publications: Racine, WI, USA, 1994; ISBN 13-978-0966020700.

18. Mussa, M.H.; Rahaq, Y.; Takita, S.; Zahoor, F.D.; Farmilo, N.; Lewis, O. The Influence of Adding a Functionalized Fluoroalkyl Silanes (PFDTES) into a Novel Silica-Based Hybrid Coating on Corrosion Protection Performance on an Aluminium 2024-t3 Alloy. *MDPI Mater. Proc.* **2021**, *7*, 6. [CrossRef]
19. Fateh, A.; Aliofkhazraei, M.; Rezvanian, A.R. Review of corrosive environments for copper and its corrosion inhibitors. *Arab. J. Chem.* **2020**, *13*, 481–544. [CrossRef]
20. Mohan, S.; Sundaraganesan, N.; Mink, J. FTIR and Raman studies on benzimidazole. *Spectrochim. Acta Part A Mol. Spectrosc.* **1991**, *47*, 1111–1115. [CrossRef]
21. Mussa, M.H.; Zahoor, F.D.; Lewis, O.; Farmilo, N. Developing a Benzimidazole-Silica-Based Hybrid Sol–Gel Coating with Significant Corrosion Protection on Aluminum Alloys 2024-T3. *Eng. Proc.* **2021**, *11*, 3. [CrossRef]
22. Usoltseva, N.V.; Korobochkin, V.V.; Balmashnov, M.A.; Dolinina, A.S. Solution Transformation of the Products of AC Electrochemical Metal Oxidation. *Procedia Chem.* **2015**, *15*, 84–89. [CrossRef]